Supporting Information for *ACS Nano*

High Performance Chemical Sensing Using Schottky-Contacted Chemical Vapor Deposition Grown Monolayer MoS_2 Transistors

Bilu Liu[+], Liang Chen[+], Gang Liu, Ahmad N. Abbas, Mohammad Fathi, Chongwu Zhou*

Department of Electrical Engineering, University of Southern California, Los Angeles, California, 90089, United States

[+] Equal contribution.

E-mail: chongwuz@usc.edu

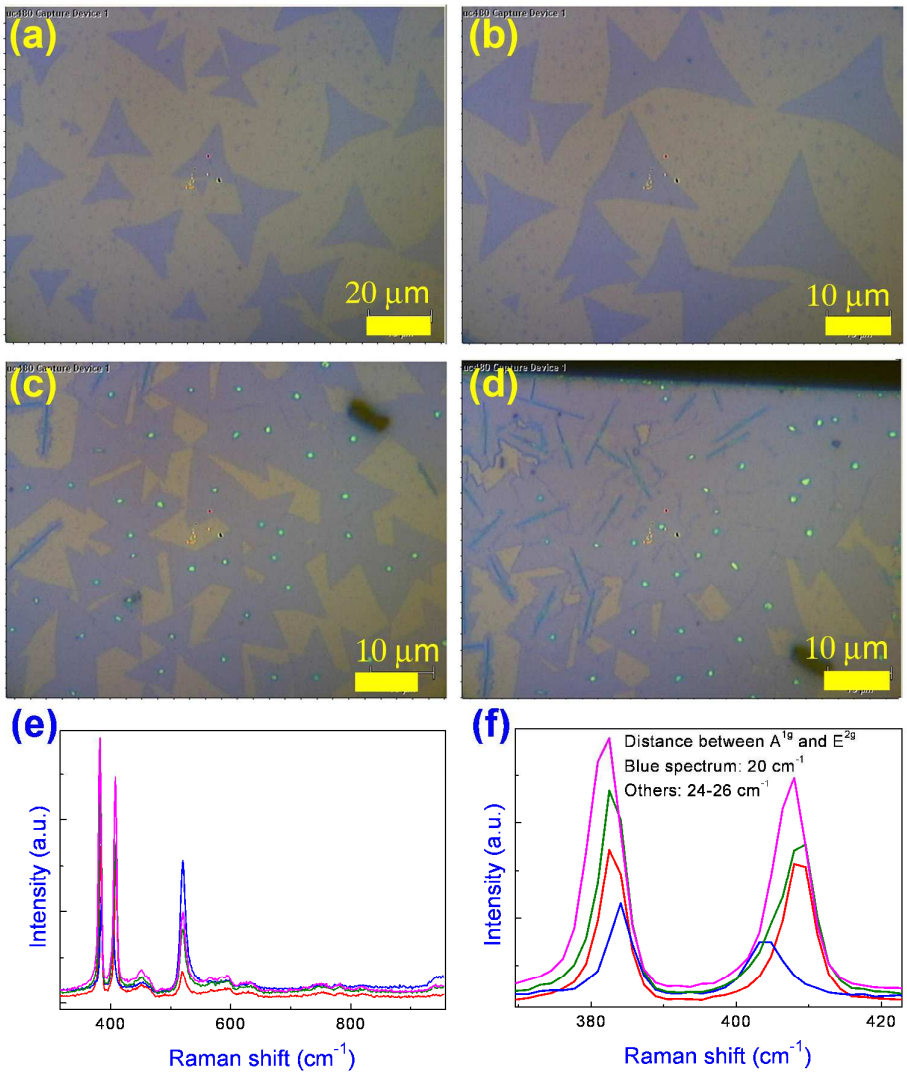

Figure S1. Optical microscopy images of as-grown MoS_2 monolayers on SiO_2/Si substrates, showing the evolution from individual triangulars (a), (b) to quasi-continuous films (c), (d). We frequently observed dots at the centers of MoS_2 sheets. (e), (f) Raman spectra of CVD grown MoS_2 and the central dots. The blue spectrum was taken at a position far away from the central dots while the other three spectra were taken at the centers of MoS_2 layers containing dots. The results show that the central dots are thick MoS_2, judging from the distance between E_{2g} and A_{1g} peaks in plot f. The spectra were taken using a 532 nm laser with spot size of ~1 μm.

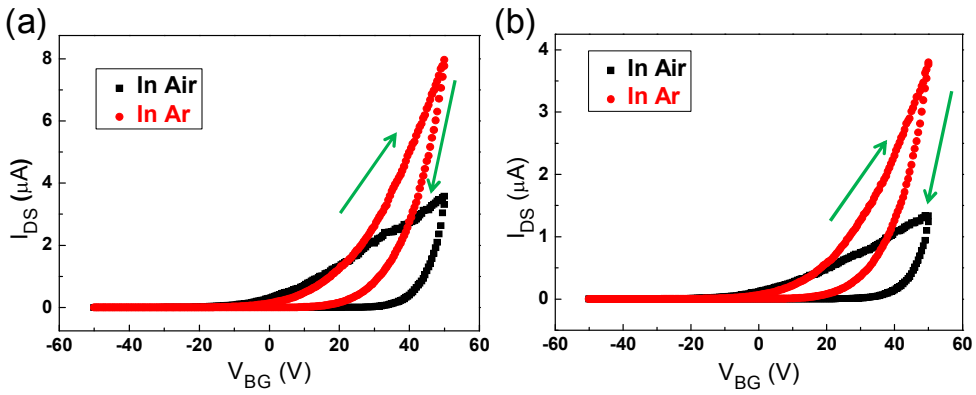

Figure S2. Transfer characteristics of two MoS_2-FETs measured in air (black) and in Ar (red). A small hysteresis and large on-state current were observed for both devices measured in Ar.

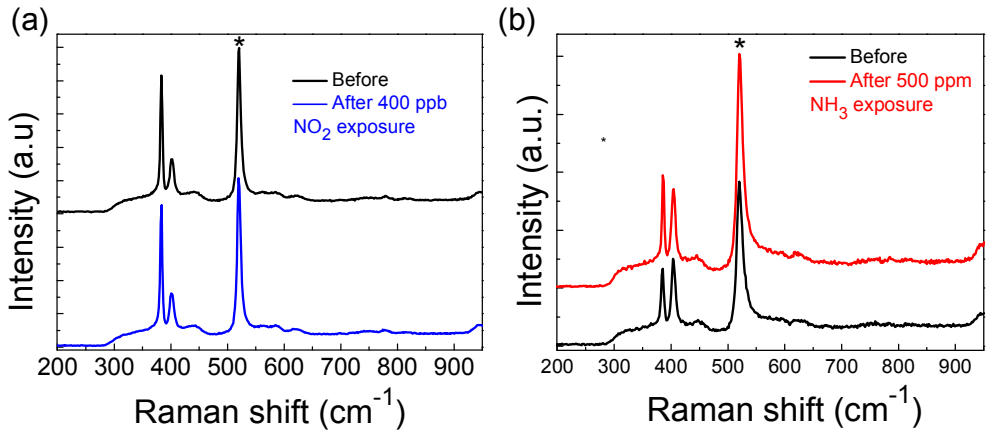

Figure S3. Raman spectra of MoS_2 sensors after exposure to 400 ppb of NO_2 (a) and 500 ppm of NH_3 (b). The spectra were vertically shifted for clarify. The peaks denoted by * at 520.7 cm^{-1} come from SiO_2/Si substrates and were used for calibration of MoS_2 Raman peaks. The excitation laser wavelength is 532 nm and the laser power is the same for all measurements.

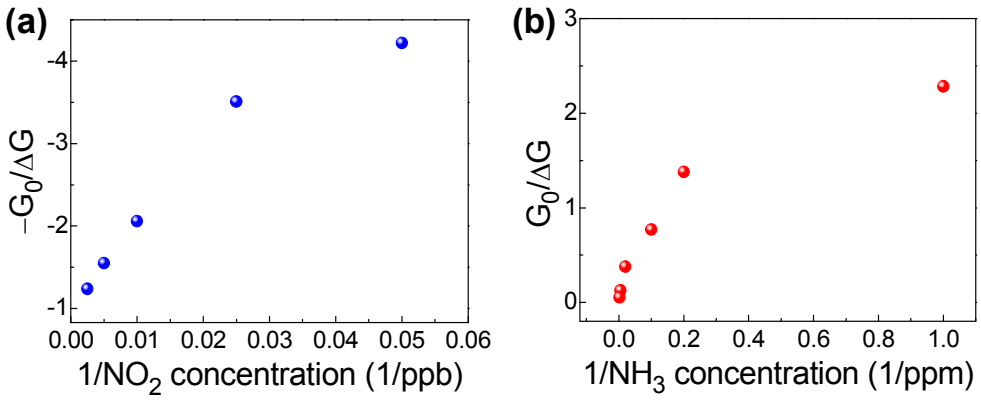

Figure S4. Plot of inverse gas concentration $(\mathrm{Conc})^{-1}$ versus inverse sensor response $(\frac{\Delta G}{G_0})^{-1}$ for NO_2 (a) and NH_3 (b).

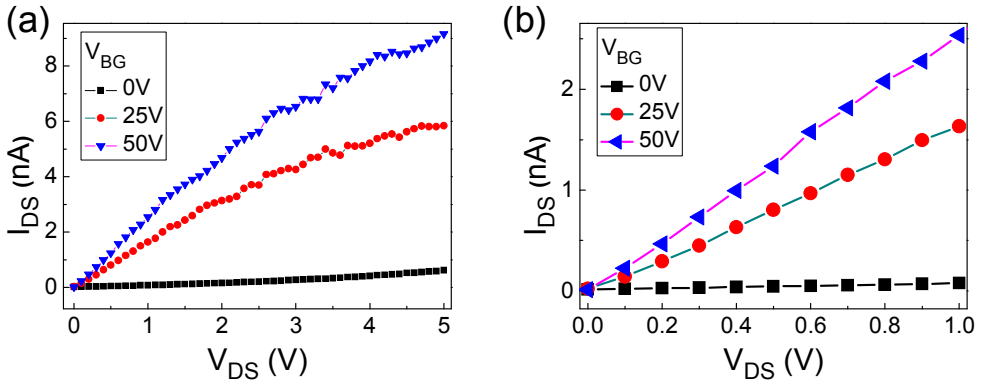

Figure S5. Output characteristics of the annealed MoS_2 device where a saturation behavior is observed in (a) and the I_{DS}-V_{DS} show linear relationship at small bias (b).

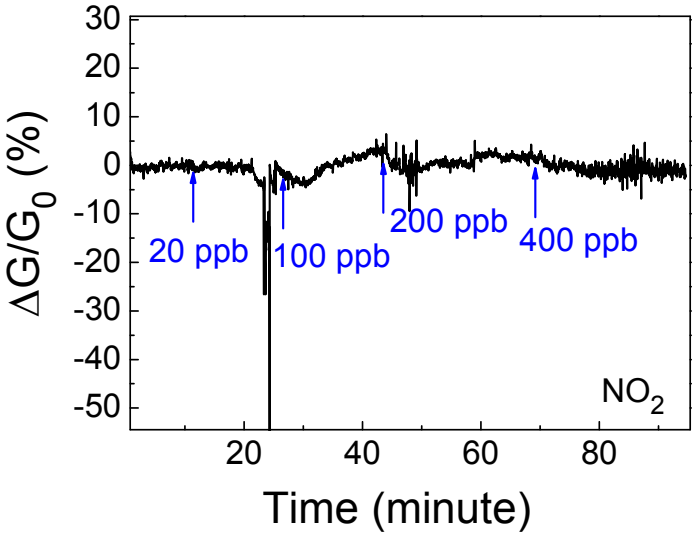

Figure S6. Real time conductance changes of an ohmic-contacted MoS_2 FET with NO_2 concentrations from 20 ppb to 400 ppb. The arrows indicate the time when certain concentrations of NO_2 were introduced. The conductance changes were smaller than 5% for 400 ppb NO_2.

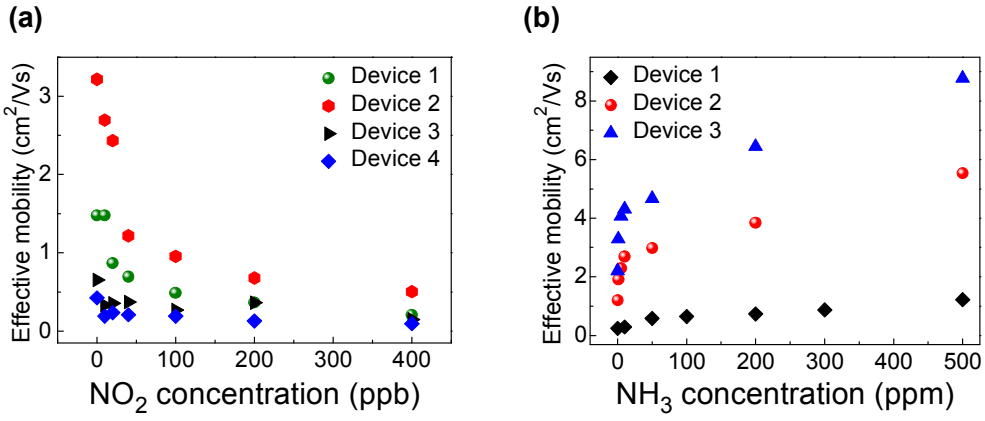

Figure S7. Effective mobility changes of the MoS_2 transistors upon exposure to NO_2 (a) and NH_3 (b) with different concentrations. The forward sweeps (V_{BG} spans from -50 V to +50 V) were used to extract the mobility.

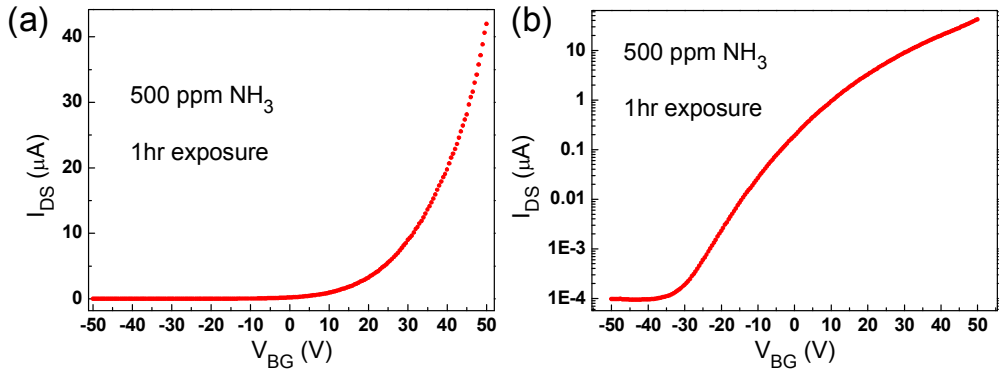

Figure S8. Transfer characteristic of a MoS_2-FET after exposure to 500 ppm NH_3 for 1 hr in linear scale (a) and log scale (b). The device shows an effective mobility up to 26.9 cm^2/Vs under a back gate configuration. The measurement was performed from 50 V to -50 V (backward sweep) for V_{BG} under a V_{DS} of 5V.